

1 **Rapid CD4 cell loss is caused by specific CRF01\_AE cluster with V3 signatures**  
2 **favoring CXCR4 usage**

3

4 **Short title: CRF01\_AE cluster with high pathogenicity**

5

6 Hongshuo Song<sup>a</sup>, Weidong Ou<sup>a</sup>, Yi Feng<sup>a</sup>, Junli Zhang<sup>a</sup>, Fan Li<sup>a</sup>, Jing Hu<sup>a</sup>, Hong Peng<sup>a</sup>,  
7 Hui Xing<sup>a</sup>, Liying Ma<sup>a</sup>, Qiuxiang Tan<sup>b</sup>, Beili Wu<sup>b</sup>, and Yiming Shao<sup>a,c,1</sup>

8

9 <sup>a</sup> State Key Laboratory for Infectious Disease Prevention and Control, National Center  
10 for AIDS/STD Control and Prevention, Chinese Center for Disease Control and  
11 Prevention, Beijing 102206, China; <sup>b</sup> Chinese Academy of Sciences, Shanghai 201203,  
12 China; <sup>c</sup> Center of Infectious Diseases, Peking University, Beijing 100191, China.

13

14 <sup>1</sup>Correspondence to:  
15 Dr. Yiming Shao, M.D., Ph.D.  
16 National Center for AIDS/STD Control and Prevention  
17 Chinese Center for Disease Control and Prevention  
18 Beijing 102206, China  
19 Phone: 86-10-82805014  
20 Email: yshao@bjmu.edu.cn

21

22

23

24

25 **Key words:** CRF01\_AE; Coreceptor tropism; CXCR4; HIV-1 pathogenesis

26

27

28

29

30

31 **Abstract**

32 HIV-1 evolved into various genetic subtypes and circulating recombinant forms (CRFs)  
33 in the global epidemic, with the same subtype or CRF usually having similar phenotype.  
34 Being one of the world's major CRFs, CRF01\_AE infection was reported to associate  
35 with higher prevalence of CXCR4 (X4) viruses and faster CD4 decline. However, the  
36 underlying mechanisms remain unclear. We identified eight phylogenetic clusters of  
37 CRF01\_AE in China and hypothesized that they may have different phenotypes. In the  
38 national HIV molecular epidemiology survey, we discovered that people infected by  
39 CRF01\_AE cluster 4 had significantly lower CD4 count (391 vs. 470,  $p < 0.0001$ ) and  
40 higher prevalence of predicted X4-using viruses (17.1% vs. 4.4%,  $p < 0.0001$ )  
41 compared to those infected by cluster 5. In a MSM cohort, X4-using viruses were only  
42 isolated from sero-convertors infected by cluster 4, which associated with rapid CD4  
43 loss within the first year of infection (141 vs. 440,  $p = 0.01$ ). Using co-receptor binding  
44 model, we identified unique V3 signatures in cluster 4 that favor CXCR4 usage. We  
45 demonstrate for the first time that HIV-1 phenotype and pathogenicity can be  
46 determined at the phylogenetic cluster level in a single subtype. Since its initial spread  
47 to human from chimpanzee in 1930s, HIV-1 remains undergoing rapid evolution in  
48 larger and more diverse population. The divergent phenotype evolution of two major  
49 CRF01\_AE clusters highlights the importance in monitoring the genetic evolution and  
50 phenotypic shift of HIV-1 to provide early warning for the appearance of more  
51 pathogenic strains such as CRF01\_AE cluster 4.

52

53

54

55 **Significance Statement**

56 Past studies on HIV-1 evolution were mainly at the genetic level. This study provides  
57 well-matched genotype and phenotype data and demonstrates disparate pathogenicity  
58 of two major CRF01\_AE clusters. While both CRF01\_AE cluster 4 and cluster 5 are  
59 mainly spread through the MSM route, cluster 4 but not cluster 5 causes fast CD4 loss,  
60 which is associated with the higher prevalence CXCR4 viruses in cluster 4. The higher  
61 CXCR4 use tendency in cluster 4 is derived from its unique V3 loop favoring CXCR4  
62 binding. This study for the first time demonstrates disparate HIV-1 phenotype between  
63 different phylogenetic clusters. It is important to monitor HIV-1 evolution at both the  
64 genotype and phenotype level to identify and control more pathogenic HIV-1 strains.

65

66

67

68

69

70

71

72

73

74

75

76

77

78 **Introduction**

79 During global transmission, HIV-1 evolved into various subtypes and their hybrids, the  
80 so called circulating recombinant forms (CRFs) (1). CRF01\_AE, one of the major CRFs  
81 spreads mainly in Southeast Asia and China (1, 2). Early studies in Thailand reported  
82 faster CD4 loss and shorter survival of CRF01\_AE infected people compared to  
83 infections in western countries where subtype B predominate (3-6). In recent years,  
84 faster disease progression of CRF01\_AE was also reported in China (7-9). Although  
85 past studies reported high prevalence of X4 viruses and fast disease progression of  
86 CRF01\_AE infections (7, 8, 10, 11), the data were mainly based on samples without  
87 known infection time and genotypic prediction without phenotypic confirmation. It is still  
88 unclear how early X4 viruses can emerge during natural CRF01\_AE infection and  
89 whether the genotypic prediction is reliable.

90

91 The epidemic of CRF01\_AE in China was initiated by multiple phylogenetic clusters  
92 introduced from Thailand in 1990s (2). We formerly identified eight CRF01\_AE clusters,  
93 which have different geographic distributions and epidemic patterns (2, 12). Therefore,  
94 we hypothesized that they may have different phenotypes. We used the national HIV  
95 molecular epidemiology survey (NHMES) dataset for screening and a men-who-have-  
96 sex-with-men (MSM) sero-incidence cohort for in-depth study to determine the time of  
97 X4 virus emergence, and phenotypically confirmed viral tropism using matched viral  
98 isolates. We observed significantly lower CD4 counts in CRF01\_AE cluster 4 compared  
99 to cluster 5 in the NHMES dataset. Focusing on the MSM cohort, we demonstrated  
100 higher prevalence of X4 phenotype in cluster 4 among people within the first year of



101 infection. We further determined the genetic and structural basis favoring X4 co-  
102 receptor usage in cluster 4. This is the first demonstration that different clusters from the  
103 same HIV-1 subtype can cause disparate rate of disease progression and bridged the  
104 missing link between CRF01\_AE genetic makeup, phenotype and clinical outcomes.

105

106

## 107 **Results**

### 108 **Lower CD4 T cell count and higher prevalence of X4-using virus in CRF01\_AE** 109 **cluster 4**

110 We compared the CD4 T cell counts of 1118 CRF01\_AE, 633 CRF07\_BC and 123  
111 subtype B newly diagnosed HIV-1 positive participants in the China's NHMES study and  
112 found no differences (Fig. 1A). When analyzing the two major CRF01\_AE clusters  
113 which contribute greatly to China's MSM epidemic, however, the CD4 count in cluster 4  
114 was significantly lower than in cluster 5 ( $p < 0.0001$ ) (Fig. 1B). Since CD4 counts  
115 decline with time during natural infection, we distinguished cases of recent infection  
116 from long-term infection by HIV-1 Limiting Antigen-Avidity assay. Significantly lower  
117 CD4 count in cluster 4 was found in both recent and long-term infection groups ( $p =$   
118  $0.0004$  and  $p < 0.0001$ , respectively) (Fig.1C-D). The proportion of people with CD4  
119 below 200 was higher in cluster 4 than in cluster 5 (9.2 % vs.1.8 %,  $p = 0.0001$ ) (Fig.  
120 1B), while the rates of recent infection were nearly the same between the two clusters  
121 (31.3% vs. 31.4%). The results clearly showed that the CRF01\_AE cluster 4 but not  
122 cluster 5 leads to rapid CD4 cell loss after infection.

123 Because CXCR4 tropism is associated with lower CD4 cell count (13-17), we  
124 investigated the prevalence level of X4 viruses in clusters 4 and 5 using genotypic  
125 prediction. Geno2pheno prediction (FPR cutoff = 2%) showed higher prevalence of X4  
126 genotype in cluster 4 than in cluster 5 (17.1% vs. 4.4%,  $p < 0.0001$ ) (Fig. 1E). In cluster  
127 4, the X4 genotype were “concentrated” among patients with low CD4 counts (Fig. 1E).  
128 This result indicates a strong association between higher X4 prevalence and lower CD4  
129 count in CRF01\_AE cluster 4 infection.

130

### 131 **High prevalence of X4-using phenotype in CRF01\_AE cluster 4 among recently** 132 **infected individuals**

133 To further characterize the mechanism of fast CD4 cell loss in CRF01\_AE cluster 4, we  
134 focused on a sero-incidence cohort with around two thousands of MSMs from Beijing  
135 Chaoyang District (the CYM cohort). For the 135 MSM sero-convertors, we first  
136 performed Illumina deep sequencing on all 78 participants with archived first year blood  
137 samples and successfully sequenced 71 of them, with an average of 65,000 sequencing  
138 reads per participant (SI Appendix, Figs. S1-S2, Tables S1-S2). Analysis of  
139 Geno2pheno FPR distribution among the plasma viral quasispecies in each participant  
140 again found higher frequency of X4-using variants in people infected by CRF01\_AE  
141 cluster 4 than by cluster 5, CRF07\_BC and subtype B (Fig. 2 and SI Appendix, Fig. S3  
142 and Table S2). Together, deep sequencing on samples collected within the first year of  
143 infection confirmed the observation in large cross-sectional NHMES study.

144 To confirm the genetic prediction phenotypically, we isolated viruses using  
145 cryopreserved PBMC from the deep sequenced CRF01\_AE participants and conducted

146 coreceptor tropism assays using GHOST cell lines. A total of 24 viruses were  
147 successfully isolated. Five showed X4-using phenotype and the remaining 19 were R5-  
148 only phenotype (Fig. 3A-C). All of the five isolates with X4-using phenotype, including  
149 four dual-tropic and one exclusively X4-tropic belonged to cluster 4 (Fig. 3A and SI  
150 Appendix, Fig. S4) (The method to determine coreceptor tropism was described in  
151 Materials and Methods and Fig. S4). This indicates a much higher prevalence of X4-  
152 using phenotype in cluster 4 than in cluster 5 (31.3% vs. 0%), consistent with the result  
153 of genotypic prediction.

154

#### 155 **Individuals harboring X4 viruses had significantly lower CD4 T cell count**

156 Previous studies demonstrated the association between X4-using phenotype and lower  
157 CD4 count, mainly for subtype B HIV-1 (13-17). However, a recent study based solely  
158 on genotypic prediction failed to find such an association in CRF01\_AE infected people  
159 in China (though there is a trend that people with CD4<50 tend to have Geno2pheno  
160 FPR<5) (8). Because genotypic prediction could overestimate the actual X4 prevalence,  
161 we therefore compared the CD4 T cell count base on virus phenotype (Fig. 3D). Among  
162 the 24 phenotype-confirmed participants, those with X4-using phenotype had  
163 significantly lower CD4 counts compared to those with R5-only phenotype in cluster 4  
164 (141 vs. 440,  $p = 0.003$ ) and in cluster 5 (141 vs. 441,  $p = 0.01$ ) (Fig. 3A and 3D). With  
165 well-matched phenotype data, we confirmed that X4-using phenotype is associated with  
166 significantly lower CD4 count in CRF01\_AE. The higher prevalence of X4 phenotype in  
167 cluster 4 during the first year of infection and its association with lower CD4 count

168 explained the reason why cluster 4 had lower CD4 count compared to cluster 5 starting  
169 from early infection stage (Fig. 1C-D).

170

### 171 **Genetic and structural determinants for higher CXCR4 usage propensity**

172 To explore the mechanism for higher X4-using propensity exhibited by cluster 4 viruses,  
173 we first compared the V3 loop sequences between clusters 4 and 5. We found that  
174 cluster 4 viruses have two highly conserved basic amino acids at positions 13 and 32 in  
175 its V3 loop (R13 and K32, HXB2 numbering R308 and K327), which were present in  
176 only about 8% of the cluster 5 viruses (Fig. 4A-B). These two conserved amino acids  
177 confer cluster 4 viruses a higher positively charged V3 loop, upon which fewer  
178 mutations may be required to switch from the R5 to X4 phenotype. Structure analysis  
179 using V3-docking models (18) suggested that residue R13 in cluster 4 potentially forms  
180 salt bridges with D262 and E277 and a hydrogen bond with the side chain of H281 in  
181 the CXCR4 coreceptor, while the corresponding residue in cluster 5 may form hydrogen  
182 bonds with K22 and D276 in the CCR5 coreceptor (Fig. 4C). Because the ligand binding  
183 pocket of CXCR4 is more negatively charged than that in CCR5, the positively charged  
184 residue R13 in cluster 4 viruses is more favored. The residue K32 in cluster 4 may form  
185 salt bridges with CXCR4's N terminus, which contains more acidic residues than  
186 CCR5's N terminus (Fig. 4C). Therefore, the highly conserved residues R13 and K32 in  
187 cluster 4 may be key determinants for the higher tendency of X4 usage. Interestingly,  
188 the V3 region of cluster 4 has less variations compared to the CRF01\_AE ancestor  
189 sequences from Thailand, notably the preservation of residue K32, while cluster 5 is  
190 more divergent (Fig. 4A and SI Appendix, Fig. S5).

191 Despite the fact that R13 and K32 were present in vast majority of cluster 4 viruses,  
192 only about 30% of individuals in cluster 4 were phenotypically confirmed to harbor X4  
193 viruses. This indicates the existence of additional determinants to shift to the X4  
194 phenotype. To further identify key amino acids governing the phenotype switch, we  
195 analyzed the genetic composition of PBMC isolates at the single-genome level (Fig. 5  
196 and SI Appendix, Fig. S6 and Table S3). In order to “sieve out” the X4-using variant(s)  
197 from the entire viral population (that is, the exact sequence(s) accounting for the X4-  
198 using phenotype), we further sequenced the viruses released from the GHOST.X4 cell  
199 culture by SGA for the five X4-using samples (SI Appendix, Table S3). Comparing the  
200 genetic composition between the PBMC viral isolates and the concurrent plasma viral  
201 population showed two different patterns: in majority of R5 subjects (15 of 19), the V3  
202 lineages in the PBMC isolate and in plasma were in proportion, that is, the predominant  
203 lineage in the PBMC isolate was also the predominant one in plasma (Fig. 5A and SI  
204 Appendix, Table S3). In contrast, in four of the five X4 isolates (with the exception of  
205 CYM194), the predominant, phenotypically confirmed X4 lineage in the PBMC isolate  
206 existed as minor variant in plasma (Fig. 5B and SI Appendix, Table S3). All V3 lineages  
207 detected in the viral isolates from PBMC were present in plasma, and more V3 lineages  
208 were detected in plasma than in the primary isolates (Fig. 5 and SI Appendix, Table S3).  
209  
210 Several V3 alterations were found in the phenotypically confirmed X4 sequences. First,  
211 all X4-using sequences lost the N-linked glycan site at the beginning of the V3 loop (V3  
212 positions 6-8, HXB2 numbering 301-303), mostly by T to I substitution at position 8 (Fig.  
213 6A). Second, while residue N was invariably found in all R5 sequences at position 7, all

214 but one X4-using sequences had residue K at this position (Fig. 6A). Third, either E or D  
215 were found at position 25 in R5 sequences, however, non-E/D substitutions (S/A/G)  
216 were present in majority of X4-using sequences (Fig. 6A). Interestingly, none of the X4  
217 sequences have positively charged amino acid R or K at V3 position 11 or 25, which are  
218 important for X4 usage in other HIV-1 subtypes (19-21). This implies different  
219 evolutionary pathway of coreceptor switching in CRF01\_AE HIV-1. In genotypic  
220 prediction, all X4-using sequences had Geno2pheno FPR values below 2%, and V3 net  
221 charge no less than 5. In contrast, all R5 sequences had FPR values higher than 2%,  
222 and V3 net charge no more than 5. As expected, cluster 4 has an overall higher V3 net  
223 charge than cluster 5 (Fig. 6A). Notably, five sequences in cluster 4 with FPR below 5%  
224 were in fact R5-only phenotype (Fig. 6A). Therefore, using FPR 5% as the cutoff may  
225 significantly overestimate the prevalence of X4 phenotype in CRF01\_AE.

226

227 Using the CCR5-V3 and CXCR4-V3 complex models (22, 23) , we also investigated the  
228 role of V3 positions 7, 8 and 25 in viral tropism from a structural perspective. In the  
229 model of CCR5-V3 complex, residue T8 in R5 V3 loop is surrounded by hydrophilic  
230 amino acids, suggesting that residue T8 is more favored by hydrophilic environment.  
231 However, in the model of CXCR4-V3 complex, residue I8 in the X4 V3 loop is  
232 surrounded by hydrophobic amino acids (Fig. 6B). This could explain why all X4 viruses  
233 have T to I/M substitutions at position 8 because the residue T8 may not well fit the  
234 hydrophobic environment within CXCR4's ligand binding pocket. In the CXCR4-V3  
235 complex, V3 position 7 is surrounded by negatively charged residues, which favor the  
236 interaction with positively charged residues K7 in X4 sequences (Fig. 6B). Compared to

237 the corresponding region in the ligand binding pocket of CXCR4, the ligand binding  
238 pocket in CCR5 around V3 position 25 contains more positively charged residues,  
239 which are favored for interacting with the negatively charged residues D/E25. This  
240 explained why all R5 viruses have D/E at V3 position 25. However, D/E may be less  
241 favored in the less positively charged environment in the ligand binding pocket of  
242 CXCR4 (Fig. 6B). Therefore, non-D/E substitutions as observed in X4-using sequences  
243 would be required for efficient X4 binding (Fig. 6B). Taken together, genetic analysis in  
244 combination with structural modeling showed that specific V3 substitutions at position 7,  
245 8 and 25 may be required to achieve X4-using phenotype in the context of CRF01\_AE  
246 cluster 4 envelope.

247

## 248 **Discussion**

249 Since the initial introduction to human in the early 20th century, HIV-1 evolved  
250 genetically and biologically with faster pace than other viruses, due to both the high  
251 error-prone nature of its reverse transcriptase and the unusual transmission routes,  
252 such as drug injections, heterosexual transmission and MSM activities. The Chinese  
253 HIV-1 epidemic with multiple subtypes and their genetic clusters circulating at the same  
254 time provides a unique opportunity to monitor virus evolution at both the genotype and  
255 phenotype levels.

256

257 Past studies on HIV-1 evolution were mainly focused on virus genotype not phenotype,  
258 because the later takes longer observation time and requires large well-matched  
259 samples. In this study, we focused on various genetic clusters of CRF01\_AE HIV-1 in

260 China. In the large cross sectional data from the NHMES, we discovered significant  
261 difference in CD4 count between people infected by CRF01\_AE cluster 4 and 5, at both  
262 early and later stage of infection. The lower CD4 count in cluster 4 is directly associated  
263 with the higher prevalence of X4 virus based on genotypic prediction. This genotype-  
264 based observation in large population was further confirmed by well-matched  
265 genotyping and phenotyping data from a MSM sero-incidence cohort. We observed that  
266 among sero-convertors, those harboring X4-using viruses had rapid CD4 loss.

267

268 It is usually considered that X4 variants emerge during late stage of infection, with the  
269 development of immunodeficiency of the host (24). In subtype B HIV-1, around 50% of  
270 patients underwent coreceptor switch, usually after 5 years of infection, which correlated  
271 with rapid CD4 decline and faster progression to AIDS (16, 25-30). The exact time of  
272 coreceptor switch in different HIV-1 subtypes are not well understood. A recent study  
273 did not detect X4 variants in subtype B infected people who were within 2 years of  
274 infection (31). We demonstrated here that in certain HIV-1 subtypes or clusters, such as  
275 CRF01\_AE cluster 4, coreceptor switch can occur much earlier than previously thought.  
276 This unusually fast speed of coreceptor switch is associated with the rapid CD4 loss in  
277 CRF01\_AE cluster 4 compared to cluster 5 as well as other HIV-1 subtypes. Supported  
278 by genetic and structural analysis, the unique V3 signatures in cluster 4 (R13 and K32),  
279 which confer higher V3 net charge may be the major intrinsic determinant for such a  
280 high coreceptor switch tendency. Further efforts are required to understand whether the  
281 rapid emergence of X4 virus in vivo is essentially a random event due to accumulation  
282 of mutations, or also driven by host factor(s) like immune pressure. In addition,



283 envelope positions outside of the V3 loop like V1V2 could also play a part in this  
284 process. A better understanding of the driving force and evolutionary pathway for  
285 coreceptor switch in CRF01\_AE cluster 4 may lead to strategies to block the early  
286 emergence of X4 virus during infection.

287

288 The genetic features of the X4 variants in CRF01\_AE cluster 4 are also different from  
289 previously found in other HIV-1 subtypes. In particular, none of the X4 sequences in  
290 CRF01\_AE cluster 4 have positively charged amino acid (R or K) at V3 positions 11 or  
291 25, which are key amino acids for X4 usage observed in other subtypes (19-21). Instead,  
292 all of them lost the V3 glycan (the N301 glycan), and nearly all have residue K at V3  
293 position 7. This highlights different evolutionary pathways for coreceptor switching in  
294 different HIV-1 subtypes. N301 glycan has previously been shown to be functionally  
295 critical for both coreceptor utilization and virus replication in subtype B (32, 33). With  
296 compensatory mutations or a high V3 net charge, loss of the N301 glycan leads to  
297 switch from R5 to X4 phenotype (32, 33). However, in the absence of compensatory  
298 mutations, loss of this glycan can abolish virus replication (32). Possibility due to this  
299 high fitness constraint, N301 glycan is highly conserved in naturally occurring subtype B  
300 sequences. A recent study found that in the Los Alamos HIV database, N301 glycan is  
301 present in as high as 99% of subtype B sequences with R5 phenotype and more than  
302 80% of sequences with X4 phenotype. Differently, in CRF01\_AE, 94% of R5 sequences  
303 and 39% of X4 sequences have the N301 glycan site (34). This again indicates that loss  
304 of the N301 glycan is an important pathway for coreceptor switch in CRF01\_AE HIV-1,  
305 but is not a primary route among subtype B viruses. It will be interesting to study in the

306 future whether N301 glycan has a lower fitness barrier in the context of CRF01\_AE  
307 cluster 4 envelope than in CRF01\_AE cluster 5 and other HIV-1 subtypes.

308

309 Another interesting finding is the outgrowth of highly replication competent X4 variants  
310 in primary viral isolates from CRF01\_AE cluster 4. The low frequency of those X4  
311 variants in plasma may not be explained by their low replication fitness, as they rapidly  
312 outcompete other lineages in the in vitro setting. Instead, it is more likely due to the  
313 compartmentalization of the R5 and X4 viruses in different cell subsets or tissues in vivo.  
314 Due to the differential expressions of CCR5 and CXCR4 coreceptors in memory and  
315 naïve CD4 T cell subsets (35, 36), R5 and X4 viruses are considered to preferentially  
316 replicate in the memory and naïve CD4 subsets, respectively (37-41). It has been  
317 shown that naïve CD4 T cells produce viruses at a lower propagation rate than memory  
318 T cells (42, 43), possibility due to the relatively low division rate (44, 45). Therefore, in  
319 vivo, those minor X4 lineages might compartmentalize in cell subsets or tissues that  
320 shut the viruses less efficiently into the blood. Regardless of the mechanism, this  
321 observation has its clinical implication: because conventional sequencing method may  
322 not be sensitive enough to capture those minor X4 variants in plasma, deep sequencing  
323 or phenotypic assay would be required to determine the existence of X4 variants in vivo,  
324 especially when using treatment regimens including the CCR5 inhibitor.

325

326 In summary, we for the first time demonstrated that various phylogenetic clusters of the  
327 same HIV-1 subtype can have disparate pathogenicity and cause different disease  
328 outcomes, which filled the missing link between HIV-1 phylogenetic cluster and viral

329 phenotype. At the phenotype level, CRF01\_AE cluster 4 evolved enhanced X4 tropism  
330 and viral pathogenesis, while cluster 5 became more attenuated due to a decreased  
331 potential of using CXCR4. Whether the process of “phenotype divergence” occurred as  
332 a random founder event from the initial seeding clusters, or due to adaptation to  
333 different hosts or transmission routes remains to be studied. Our study emphasizes the  
334 importance of monitoring HIV-1 genetic drift and phenotype shift at the phylogenetic  
335 cluster level in order to timely control the spread of more pathogenic viruses like  
336 CRF01\_AE cluster 4.

337

338

## 339 **Materials and Methods**

### 340 **Study participants**

341 The study participants were from the national HIV molecular epidemiology survey  
342 (NHMES) and the Beijing Chaoyang District MSM cohort (the CYM cohort). Written  
343 informed consent was obtained from all study participants. See SI Appendix,  
344 Supplementary Text for details.

345

### 346 **Enzyme Immunoassay (EIA)**

347 In order to distinguish recent HIV-1 infections from long-term HIV-1 infections, the  
348 Enzyme Immunoassay (EIA) was performed using the Maxim HIV-1 Limiting Antigen-  
349 Avidity (LAg-Avidity) EIA kit (Maxim Biomedical). The experiment and data analysis  
350 were performed according to manufacturer’s instructions (Maxim Biomedical).

351

352 **Viral RNA extraction and cDNA synthesis**

353 Viral RNA was extracted from 200 µl of plasma sample using the QIAamp Viral RNA  
354 Mini Kit (Qiagen). RNA was eluted into 50 µl of RNase free water. A total of 17 µl viral  
355 RNA was used for cDNA synthesis using the SuperScript III reverse transcriptase  
356 (Invitrogen) with the Oligo (dT) primer. The cDNA was immediately used for PCR  
357 amplification.

358

359 **Library preparation for sequencing on Illumina MiSeq**

360 The Illumina MiSeq library was prepared using a nested PCR approach. The 8 nt  
361 Illumina index and adaptors (P5 and P7) were added to both ends of the second round  
362 PCR primers (SI Appendix, Fig. S2 and Table S4). The second round PCR products  
363 were gel-purified to remove unspecific bands and primer dimers, and quantified by  
364 qPCR using the KAPA SYBR FAST qPCR kit according to manufacturer's instructions  
365 (KAPA Biosystems). See SI Appendix, Supplementary Text for details.

366

367 **Next generation sequencing and data analysis**

368 The pooled DNA library was sequenced on an Illumina MiSeq using the MiSeq Reagent  
369 Kit v2 (500 cycles, Illumina) as previously described (46). Each pair of fastq reads in  
370 files "read 1" and "read 2" were merged by the FLASH software (47). The merged fastq  
371 files were then filtered based on data quality on the Galaxy server (48) using the  
372 following parameter: no more than 10 bases with Q score lower than 30 in each read.  
373 The filtered clean reads were then converted into fasta format. In each individual,  
374 identical reads were collapsed into haplotypes after the primer regions were trimmed.

375 The frequency of each haplotype among the total clean reads was calculated. The most  
376 frequent haplotype in each individual was used to infer the phylogenetic relationship  
377 among all deep sequenced individuals.

378

### 379 **Genotypic prediction of co-receptor usage**

380 Genotypic prediction of co-receptor usage was performed using the Geno2pheno clonal  
381 model (<https://coreceptor.geno2pheno.org>) (49). For the deep sequencing data, the  
382 FPR (false positive rate, the probability of classifying an R5-virus falsely as X4) was  
383 obtained for each V3 haplotype. To avoid the impact of potential PCR or sequencing  
384 error on data analysis, only V3 haplotypes appeared three times or more in each  
385 sample were used for analysis, while V3 singletons and those appeared only twice  
386 were discarded. The frequency distribution of FPR value in each sample was obtained  
387 by calculating the frequency of each V3 haplotype among the total reads analyzed.

388

### 389 **Primary virus isolation from PBMC**

390 To obtain primary virus isolates, cryopreserved PBMC from HIV-1 infected patients  
391 were co-cultivated with stimulated normal PBMC from healthy donors. In brief, fresh  
392 PBMC from healthy donors were stimulated for 3 days in RPMI1640 containing 10%  
393 fetal bovine serum (FBS), interleukin 2 (IL-2) (32 U/ml; PeproTech), soluble anti-CD3  
394 (0.2 µg/ml; eBioscience) and soluble anti-CD28 (0.2 µg/ml; eBioscience) as described  
395 previously(50). After stimulation, cells were washed twice with RPMI1640 to remove the  
396 residue simulating antibodies. A total of  $10^7$  stimulated PBMC from healthy donor were  
397 then mixed with  $10^7$  of PBMC from an infected patient. The cell mixtures were then

398 depleted for CD8 T cells using the EasySep Human CD8 Positive Selection Kit  
399 (Stemcell Technologies). The CD8-depleted cell mixture was cultured in a T25 flask with  
400 RPMI1640 containing 10% fetal bovine serum (FBS) and 32 U/ml IL-2 (PeproTech) for  
401 up to 4 weeks. Every 3 days, half volume of the culture supernatant was replaced with  
402 fresh medium. Every 7 days, half of the entire culture (including cells) was removed,  
403 and  $5 \times 10^6$  of stimulated, CD8 T cell depleted PBMC from healthy donors were added.  
404 The p24 concentration in the culture supernatant was measured every week. Majority of  
405 cultures achieved peak p24 production around week 3. Cultures with p24 concentration  
406 less than 2 ng/ml at week 4 were considered to be failed.

407

#### 408 **Coreceptor tropism determination**

409 Coreceptor tropism of the primary viral isolates was determined using the  
410 GHOST(3).CCR5 and GHOST(3).CXCR4 cell lines (51). Both GFP expression in the  
411 Ghost cell lines and viral p24 production were used to determine the coreceptor usage.  
412 See SI Appendix, Supplementary Text for details.

413

#### 414 **Single genome amplification**

415 Single genome amplification (SGA) was performed as previously described (52). The  
416 sequences were aligned using GeneCutter  
417 ([https://www.hiv.lanl.gov/content/sequence/GENE\\_CUTTER/cutter.html](https://www.hiv.lanl.gov/content/sequence/GENE_CUTTER/cutter.html)), followed by  
418 the manual adjustment to obtain the optimal alignment. See SI Appendix,  
419 Supplementary Text for details.

420

421 **Statistical analysis**

422 All statistical analysis was performed using the Prism 7 (GraphPad Software). Statistical  
423 differences were determined using two-tailed Mann-Whitney test or Fisher's exact test  
424 as indicated in the figure legends. The exact  $p$  values were provided in the figures.

425

426 **Data availability**

427 Newly generated nucleic acid sequences in the current study were deposited in  
428 GenBank with accession numbers MH672692-MH673032.

429

430 **Acknowledgements**

431 We thank Dr. Cecilia Cheng-Mayer for comments on the manuscript. This work was  
432 supported by China National Major Project for Infectious Diseases Control and  
433 Prevention, and China Key Project of the State Key Laboratory of Infectious Diseases  
434 Control and Prevention.

435

436 **Author contributions**

437 YS conceived and designed the study. HS, WO, YF, JZ, FL, JH and HP performed  
438 experiments. QT and BW designed and performed the structural analysis. HS, WO, YF,  
439 HX, LM, QT, BW and YS analyzed the data. HS, BW and YS wrote and edited the  
440 manuscript.

441

442 **Competing interests**

443 The authors declare no competing interests.

444

445

446

447

448

449 **References :**

- 450 1. Taylor BS, Sobieszczyk ME, McCutchan FE, & Hammer SM (2008) The  
451 challenge of HIV-1 subtype diversity. *N Engl J Med* 358(15):1590-1602.
- 452 2. Feng Y, *et al.* (2013) The rapidly expanding CRF01\_AE epidemic in China is  
453 driven by multiple lineages of HIV-1 viruses introduced in the 1990s. *AIDS*  
454 27(11):1793-1802.
- 455 3. Kilmarx PH, *et al.* (2000) Disease progression and survival with human  
456 immunodeficiency virus type 1 subtype E infection among female sex workers in  
457 Thailand. *J Infect Dis* 181(5):1598-1606.
- 458 4. Costello C, *et al.* (2005) HIV-1 subtype E progression among northern Thai  
459 couples: traditional and non-traditional predictors of survival. *Int J Epidemiol*  
460 34(3):577-584.
- 461 5. Nelson KE, Costello C, Suriyanon V, Sennun S, & Duerr A (2007) Survival of  
462 blood donors and their spouses with HIV-1 subtype E (CRF01\_A\_E) infection in  
463 northern Thailand, 1992-2007. *AIDS* 21 Suppl 6:S47-54.
- 464 6. Rangsin R, *et al.* (2004) The natural history of HIV-1 infection in young Thai men  
465 after seroconversion. *J Acquir Immune Defic Syndr* 36(1):622-629.
- 466 7. Li X, *et al.* (2014) Evidence that HIV-1 CRF01\_AE is associated with low CD4+T  
467 cell count and CXCR4 co-receptor usage in recently infected young men who  
468 have sex with men (MSM) in Shanghai, China. *PLoS One* 9(2):e89462.
- 469 8. Li Y, *et al.* (2014) CRF01\_AE subtype is associated with X4 tropism and fast HIV  
470 progression in Chinese patients infected through sexual transmission. *AIDS*  
471 28(4):521-530.
- 472 9. Chu M, *et al.* (2017) HIV-1 CRF01\_AE strain is associated with faster HIV/AIDS  
473 progression in Jiangsu Province, China. *Sci Rep* 7(1):1570.
- 474 10. To SW, *et al.* (2013) Determination of the high prevalence of Dual/Mixed- or X4-  
475 tropism among HIV type 1 CRF01\_AE in Hong Kong by genotyping and  
476 phenotyping methods. *AIDS Res Hum Retroviruses* 29(8):1123-1128.



- 477 11. Ng KY, *et al.* (2013) High prevalence of CXCR4 usage among treatment-naive  
478 CRF01\_AE and CRF51\_01B-infected HIV-1 subjects in Singapore. *BMC Infect*  
479 *Dis* 13:90.
- 480 12. Li X, *et al.* (2017) Tracing the epidemic history of HIV-1 CRF01\_AE clusters  
481 using near-complete genome sequences. *Sci Rep* 7(1):4024.
- 482 13. Melby T, *et al.* (2006) HIV-1 coreceptor use in triple-class treatment-experienced  
483 patients: baseline prevalence, correlates, and relationship to enfuvirtide response.  
484 *J Infect Dis* 194(2):238-246.
- 485 14. Moyle GJ, *et al.* (2005) Epidemiology and predictive factors for chemokine  
486 receptor use in HIV-1 infection. *J Infect Dis* 191(6):866-872.
- 487 15. Wilkin TJ, *et al.* (2007) HIV type 1 chemokine coreceptor use among  
488 antiretroviral-experienced patients screened for a clinical trial of a CCR5 inhibitor:  
489 AIDS Clinical Trial Group A5211. *Clin Infect Dis* 44(4):591-595.
- 490 16. Koot M, *et al.* (1993) Prognostic value of HIV-1 syncytium-inducing phenotype for  
491 rate of CD4+ cell depletion and progression to AIDS. *Ann Intern Med* 118(9):681-  
492 688.
- 493 17. Brumme ZL, *et al.* (2005) Molecular and clinical epidemiology of CXCR4-using  
494 HIV-1 in a large population of antiretroviral-naive individuals. *J Infect Dis*  
495 192(3):466-474.
- 496 18. Tan Q, *et al.* (2013) Structure of the CCR5 chemokine receptor-HIV entry  
497 inhibitor maraviroc complex. *Science* 341(6152):1387-1390.
- 498 19. Huang W, *et al.* (2011) Mutational pathways and genetic barriers to CXCR4-  
499 mediated entry by human immunodeficiency virus type 1. *Virology* 409(2):308-  
500 318.
- 501 20. Berger EA, Murphy PM, & Farber JM (1999) Chemokine receptors as HIV-1  
502 coreceptors: roles in viral entry, tropism, and disease. *Annu Rev Immunol*  
503 17:657-700.
- 504 21. Ping LH, *et al.* (1999) Characterization of V3 sequence heterogeneity in subtype  
505 C human immunodeficiency virus type 1 isolates from Malawi:  
506 underrepresentation of X4 variants. *J Virol* 73(8):6271-6281.
- 507 22. Tamamis P & Floudas CA (2014) Molecular recognition of CCR5 by an HIV-1  
508 gp120 V3 loop. *PLoS One* 9(4):e95767.
- 509 23. Tamamis P & Floudas CA (2013) Molecular recognition of CXCR4 by a dual  
510 tropic HIV-1 gp120 V3 loop. *Biophys J* 105(6):1502-1514.
- 511 24. Swanstrom R & Coffin J (2012) HIV-1 pathogenesis: the virus. *Cold Spring Harb*  
512 *Perspect Med* 2(12):a007443.
- 513 25. Schuitemaker H, *et al.* (1992) Biological phenotype of human immunodeficiency  
514 virus type 1 clones at different stages of infection: progression of disease is  
515 associated with a shift from monocytotropic to T-cell-tropic virus population. *J*  
516 *Virol* 66(3):1354-1360.

- 517 26. Connor RI, Sheridan KE, Ceradini D, Choe S, & Landau NR (1997) Change in  
518 coreceptor use correlates with disease progression in HIV-1--infected individuals.  
519 *J Exp Med* 185(4):621-628.
- 520 27. Koot M, *et al.* (1999) Conversion rate towards a syncytium-inducing (SI)  
521 phenotype during different stages of human immunodeficiency virus type 1  
522 infection and prognostic value of SI phenotype for survival after AIDS diagnosis.  
523 *J Infect Dis* 179(1):254-258.
- 524 28. Verhofstede C, Nijhuis M, & Vandekerckhove L (2012) Correlation of coreceptor  
525 usage and disease progression. *Curr Opin HIV AIDS* 7(5):432-439.
- 526 29. Moore JP, Kitchen SG, Pugach P, & Zack JA (2004) The CCR5 and CXCR4  
527 coreceptors--central to understanding the transmission and pathogenesis of  
528 human immunodeficiency virus type 1 infection. *AIDS Res Hum Retroviruses*  
529 20(1):111-126.
- 530 30. Richman DD & Bozzette SA (1994) The impact of the syncytium-inducing  
531 phenotype of human immunodeficiency virus on disease progression. *J Infect Dis*  
532 169(5):968-974.
- 533 31. Zhou S, Bednar MM, Sturdevant CB, Hauser BM, & Swanstrom R (2016) Deep  
534 Sequencing of the HIV-1 env Gene Reveals Discrete X4 Lineages and Linkage  
535 Disequilibrium between X4 and R5 Viruses in the V1/V2 and V3 Variable  
536 Regions. *J Virol* 90(16):7142-7158.
- 537 32. Ogert RA, *et al.* (2001) N-linked glycosylation sites adjacent to and within the  
538 V1/V2 and the V3 loops of dualtropic human immunodeficiency virus type 1  
539 isolate DH12 gp120 affect coreceptor usage and cellular tropism. *J Virol*  
540 75(13):5998-6006.
- 541 33. Pollakis G, *et al.* (2001) N-linked glycosylation of the HIV type-1 gp120 envelope  
542 glycoprotein as a major determinant of CCR5 and CXCR4 coreceptor utilization.  
543 *J Biol Chem* 276(16):13433-13441.
- 544 34. Joshi A, *et al.* (2017) HIV-1 subtype CRF01\_AE and B differ in utilization of low  
545 levels of CCR5, Maraviroc susceptibility and potential N-glycosylation sites.  
546 *Virology* 512:222-233.
- 547 35. Bleul CC, Wu L, Hoxie JA, Springer TA, & Mackay CR (1997) The HIV  
548 coreceptors CXCR4 and CCR5 are differentially expressed and regulated on  
549 human T lymphocytes. *Proc Natl Acad Sci U S A* 94(5):1925-1930.
- 550 36. Lee B, Sharron M, Montaner LJ, Weissman D, & Doms RW (1999) Quantification  
551 of CD4, CCR5, and CXCR4 levels on lymphocyte subsets, dendritic cells, and  
552 differentially conditioned monocyte-derived macrophages. *Proc Natl Acad Sci U*  
553 *S A* 96(9):5215-5220.
- 554 37. Blaak H, *et al.* (2000) In vivo HIV-1 infection of CD45RA(+)CD4(+) T cells is  
555 established primarily by syncytium-inducing variants and correlates with the rate  
556 of CD4(+) T cell decline. *Proc Natl Acad Sci U S A* 97(3):1269-1274.

- 557 38. van Rij RP, *et al.* (2000) Differential coreceptor expression allows for  
558 independent evolution of non-syncytium-inducing and syncytium-inducing HIV-1.  
559 *J Clin Invest* 106(12):1569.
- 560 39. Nishimura Y, *et al.* (2005) Resting naive CD4+ T cells are massively infected and  
561 eliminated by X4-tropic simian-human immunodeficiency viruses in macaques.  
562 *Proc Natl Acad Sci U S A* 102(22):8000-8005.
- 563 40. Ribeiro RM, Hazenberg MD, Perelson AS, & Davenport MP (2006) Naive and  
564 memory cell turnover as drivers of CCR5-to-CXCR4 tropism switch in human  
565 immunodeficiency virus type 1: implications for therapy. *J Virol* 80(2):802-809.
- 566 41. Council OD & Joseph SB (2018) Evolution of Host Target Cell Specificity During  
567 HIV-1 Infection. *Curr HIV Res* 16(1):13-20.
- 568 42. Eckstein DA, *et al.* (2001) HIV-1 actively replicates in naive CD4(+) T cells  
569 residing within human lymphoid tissues. *Immunity* 15(4):671-682.
- 570 43. Zhang Z, *et al.* (1999) Sexual transmission and propagation of SIV and HIV in  
571 resting and activated CD4+ T cells. *Science* 286(5443):1353-1357.
- 572 44. McLean AR & Michie CA (1995) In vivo estimates of division and death rates of  
573 human T lymphocytes. *Proc Natl Acad Sci U S A* 92(9):3707-3711.
- 574 45. McCune JM, *et al.* (2000) Factors influencing T-cell turnover in HIV-1-  
575 seropositive patients. *J Clin Invest* 105(5):R1-8.
- 576 46. Williams WB, *et al.* (2015) HIV-1 VACCINES. Diversion of HIV-1 vaccine-induced  
577 immunity by gp41-microbiota cross-reactive antibodies. *Science*  
578 349(6249):aab1253.
- 579 47. Magoc T & Salzberg SL (2011) FLASH: fast length adjustment of short reads to  
580 improve genome assemblies. *Bioinformatics* 27(21):2957-2963.
- 581 48. Blankenberg D, *et al.* (2010) Manipulation of FASTQ data with Galaxy.  
582 *Bioinformatics* 26(14):1783-1785.
- 583 49. Lengauer T, Sander O, Sierra S, Thielen A, & Kaiser R (2007) Bioinformatics  
584 prediction of HIV coreceptor usage. *Nat Biotechnol* 25(12):1407-1410.
- 585 50. Song H, *et al.* (2012) Impact of immune escape mutations on HIV-1 fitness in the  
586 context of the cognate transmitted/founder genome. *Retrovirology* 9:89.
- 587 51. Vodros D, *et al.* (2001) Quantitative evaluation of HIV-1 coreceptor use in the  
588 GHOST3 cell assay. *Virology* 291(1):1-11.
- 589 52. Keele BF, *et al.* (2008) Identification and characterization of transmitted and early  
590 founder virus envelopes in primary HIV-1 infection. *Proc Natl Acad Sci U S A*  
591 105(21):7552-7557.

592  
593

594

595

596

597

598

599

600

## 601 **Figure legends**

602 **Figure 1.** Comparison of CD4 T cell count and prevalence of X4 virus in different HIV-1  
603 subtypes and CRF01\_AE clusters. (A) Comparison of CD4 T cell count between  
604 individuals infected by CRF01\_AE (n=1118), CRF07\_BC (n=633) and subtype B (n=123)  
605 from the national HIV molecular epidemiology survey. (B-D) Significantly lower CD4 T  
606 cell count among individuals infected by CRF01\_AE cluster 4 (n=308) than those  
607 infected by cluster 5 (n=273) regardless of the stage of infection (B), in the recent  
608 infection group (C), and in long-term infection group (D). The small figure in panel B  
609 shows the percentage of individuals with CD4 below 200. In each panel, the vertical line,  
610 box and whisker represents the median, upper and lower quantiles, and the 5-95  
611 percentile, respectively. The statistical difference in CD4 count between different groups  
612 was calculated using two-tailed Mann-Whitney U test. The percentage of subjects with  
613 CD4 below 200 was compared using two-tailed Fisher's exact test. (E) Prevalence of  
614 predicted X4 viruses in CRF01\_AE cluster 4 and cluster 5, and in the lower (<200) and  
615 higher (>200) CD4 groups in CRF01\_AE cluster 4. The statistical difference was  
616 determined using two-tailed Fisher's exact test.

617

618 **Figure 2.** Higher frequency of predicted X4-using variants in CRF01\_AE cluster 4  
619 identified by deep sequencing. (A) Phylogenetic relationship of 60 deep sequenced  
620 individuals from the CYM cohort. In each individual, the most frequent haplotype among  
621 the deep sequencing reads was used for phylogenetic inference. The Neighbor-joining  
622 (NJ) tree was constructed using the Kimura 2-parameter evolutionary model with 1000  
623 bootstrap replications. In the tree, the branches for CRF01\_AE cluster 4 (n=22), cluster  
624 5 (n=11), CRF07\_BC (n=19) and subtype B (n=8) were color coded. (B) Heatmap  
625 showing the frequency distribution of Geno2pheno FPR value among the deep  
626 sequencing reads in each individual. The samples in the phylogenetic tree and in the  
627 heatmap were matched.

628

629 **Figure 3.** Phenotypic characterization of primary CRF01\_AE viral isolates and the  
630 association between coreceptor tropism and CD4 count. (A) Coreceptor usage  
631 phenotype of 24 primary viral isolates from CRF01\_AE cluster 4 (n=16) and cluster 5  
632 (n=8) and the corresponding CD4 counts in each individual. (B) Determination of  
633 coreceptor tropism using GHOST.CCR5 and GHOST.CXCR4 cell lines. The GFP  
634 expression induced by one representative R5-only isolate and one X4-using isolate  
635 were shown. (C) Syncytium formation at day 12 post PBMC co-cultivation in the culture  
636 of CYM248, an isolate using CXCR4 exclusively. (D) Significantly lower CD4 count in  
637 individuals harboring X4-using viruses in CRF01\_AE cluster 4. The black vertical line  
638 represents the median CD4 count. The statistical difference was calculated using two-  
639 tailed Mann-Whitney U test.

640

641 **Figure 4.** Genetic determinants and structural basis of the higher X4-using tendency in  
642 CRF01\_AE cluster 4. (A) The frequency of each V3 amino acid was determined with a  
643 total of 385 available sequences from CRF01\_AE cluster 4, 328 available sequences  
644 from CRF01\_AE cluster 5, and 34 sequences from Thailand downloaded from the Los  
645 Alamos HIV sequence database (before the year 2000). The plots were generated  
646 using the WebLogo tool (<https://weblogo.berkeley.edu/>). (B) Pie charts showing the  
647 prevalence of positively charged amino acid K13 and R32 in CRF01\_AE cluster 4 and  
648 cluster 5. (C) Structural analysis for V3 position 13 and 32 in binding of the CCR5 and  
649 CXCR4 coreceptors using the V3-docking model.

650

651 **Figure 5.** Genetic composition of the PBMC viral isolates. (A-B) SGA-derived gp160  
652 sequences from the R5 isolate CYM179 (A) and the dual tropic isolate CYM176 (B)  
653 were shown using highlighter plot. In each sample, one sequence with the predominant  
654 V3 lineage was used as the master sequence. The synonymous and non-synonymous  
655 substitutions compared to the master sequence were shown in green and red,  
656 respectively. The corresponding V3 alignment was shown on the right, and different V3  
657 lineages were color-coded. The circle plots show the proportion of each V3 lineage in  
658 the PBMC viral isolate as detected by SGA and in the plasma as detected by deep  
659 sequencing. In CYM176, the red arrows indicate the phenotypically confirmed X4  
660 lineage.

661

662 **Figure 6.** Genetic characteristics of phenotypically confirmed X4 sequences and  
663 structural modeling for coreceptor binding. (A) V3 amino acids alignment of SGA-

664 derived sequences from the phenotype-confirmed primary viral isolates. Sequences  
665 shown in red were phenotypically confirmed X4-using sequences (that is, sequences  
666 sieved out from the GHOST.CXCR4 culture by SGA). Sequences shown in blue were  
667 the predominant V3 forms in the R5 isolates. Key V3 positions associated with X4-using  
668 phenotype were shaded in light blue. (B) Structural modeling for V3 positions 7, 8 and  
669 25 in binding of coreceptors CCR5 and CXCR4 using the V3-docking model.



# Figure 1

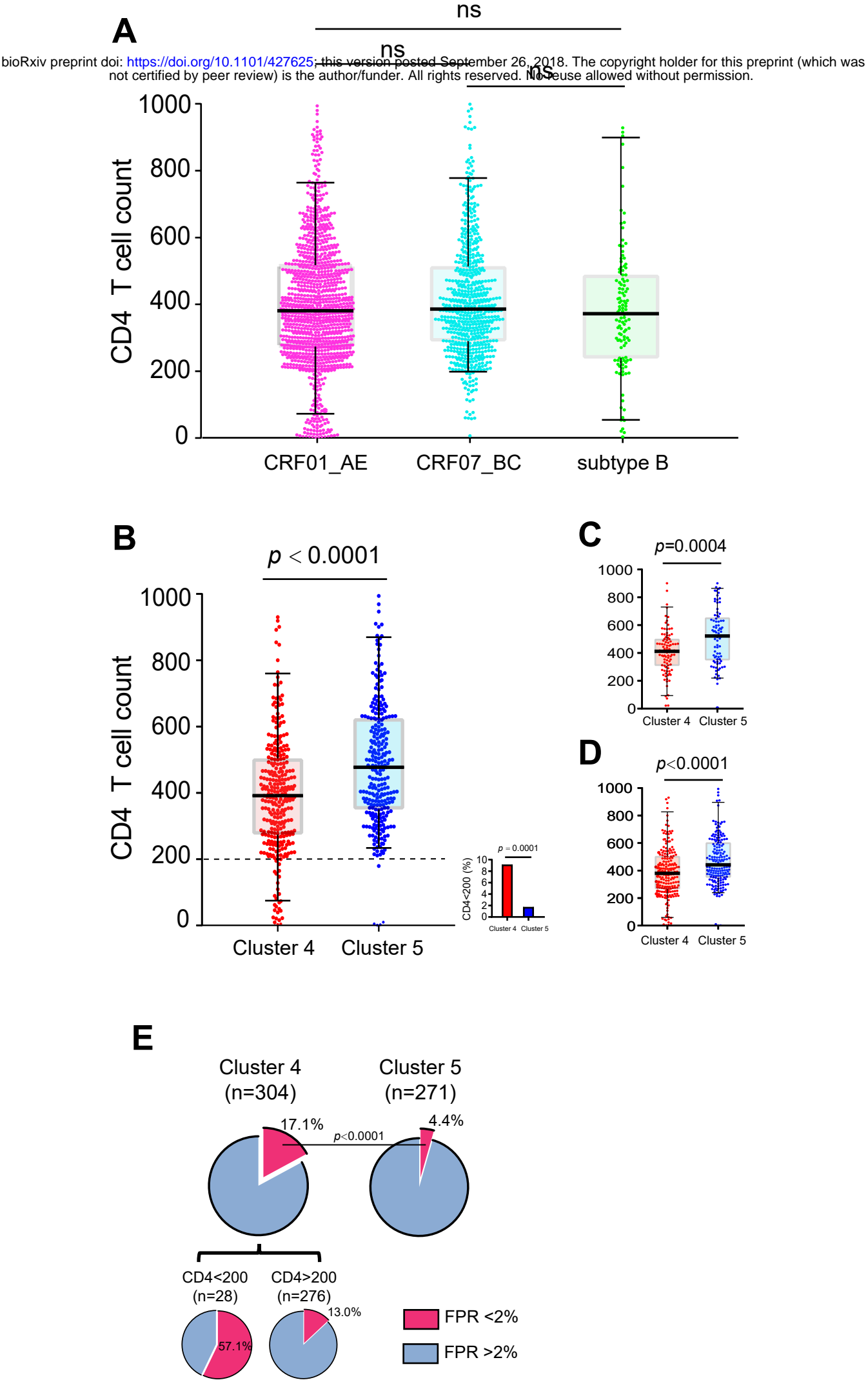
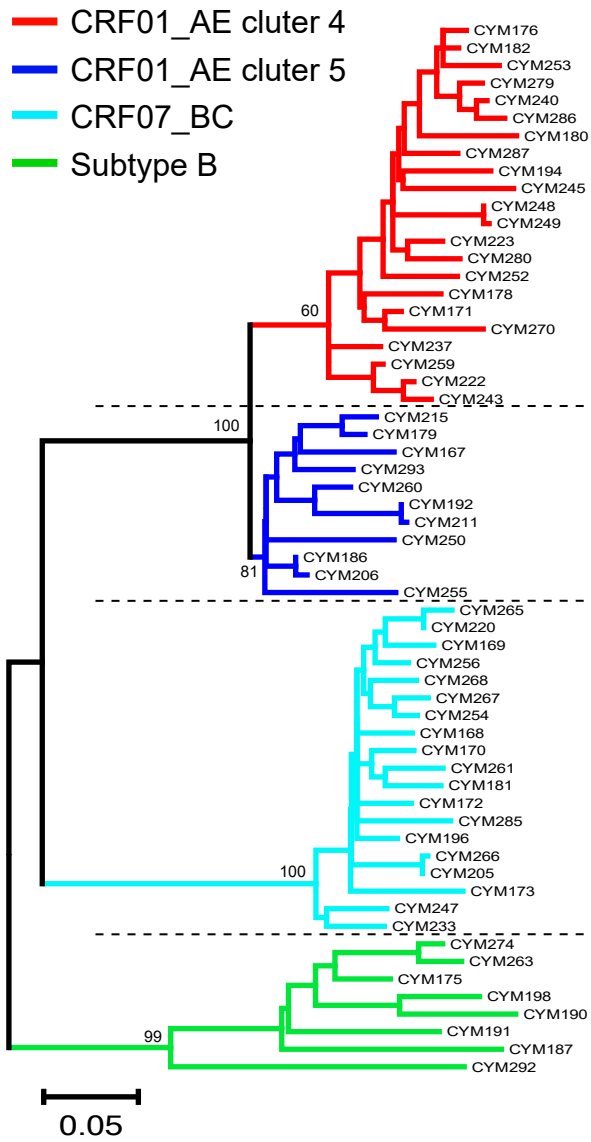




# Figure 2

bioRxiv preprint doi: <https://doi.org/10.1101/427625>; this version posted September 26, 2018. The copyright holder for this preprint (which was not certified by peer review) is the author/funder. All rights reserved. No reuse allowed without permission.

## A



## B

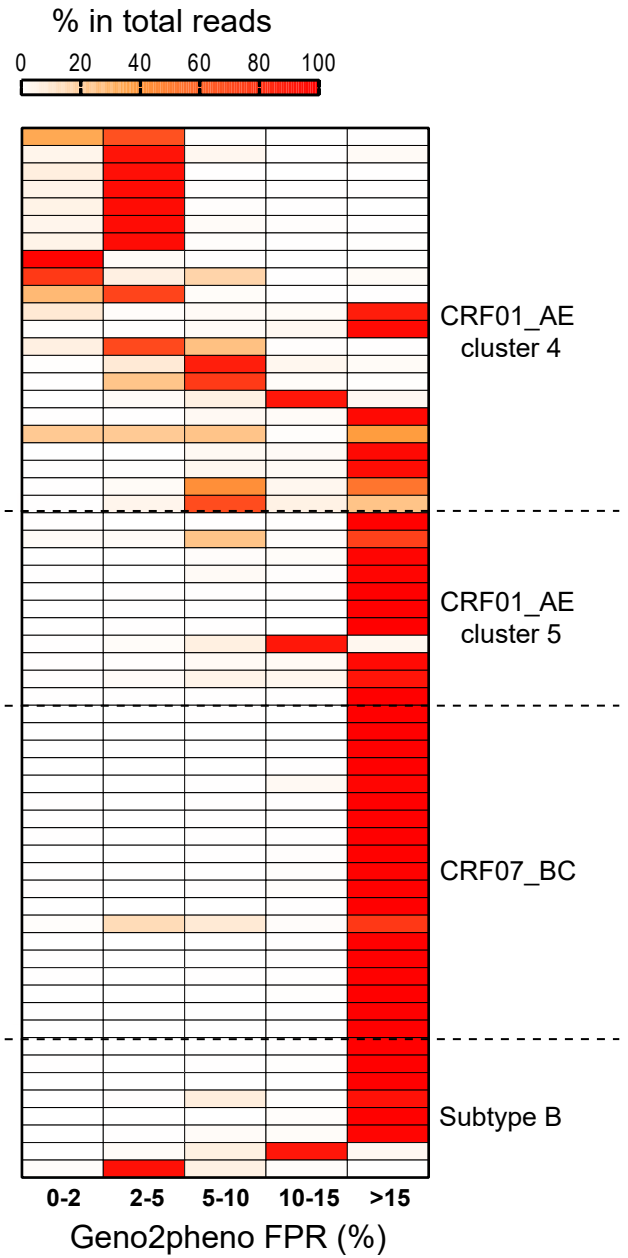
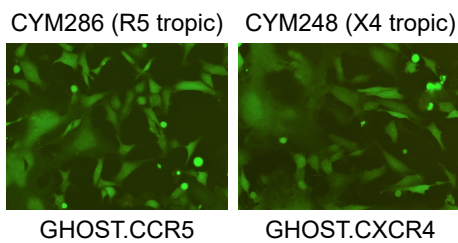


# Figure 3

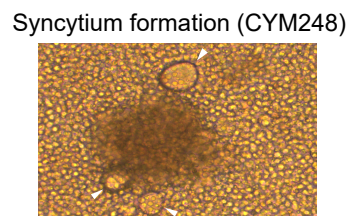
**A** bioRxiv preprint doi: <https://doi.org/10.1101/427625>; this version posted September 26, 2018. The copyright holder for this preprint (which was not certified by peer review) is the author/funder. All rights reserved. No reuse allowed without permission.

Subjects	Phenotype	CD4 count	CD4 average	
CYM248	X4	10		Cluster 4 X4-using
CYM245	R5/X4 dual	136		
CYM176	R5/X4 dual	178	141	
CYM270	R5/X4 dual	18		
CYM194	R5/X4 dual	364		
<hr style="border-top: 1px dashed black;"/>				
CYM240	R5	384		Cluster 4 R5-only
CYM286	R5	593		
CYM279	R5	402		
CYM182	R5	425		
CYM223	R5	758		
CYM249	R5	409	440	
CYM252	R5	467		
CYM178	R5	305		
CYM280	R5	347		
CYM171	R5	201		
CYM243	R5	548		
<hr style="border-top: 1px dashed black;"/>				
CYM250	R5	716		Cluster 5 R5-only
CYM293	R5	615		
CYM192	R5	348		
CYM167	R5	527	441	
CYM215	R5	416		
CYM179	R5	197		
CYM255	R5	325		
CYM186	R5	381		

**B**



**C**



**D**

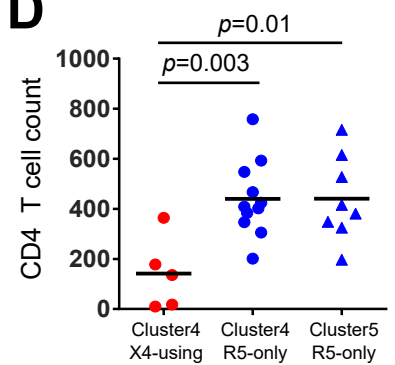
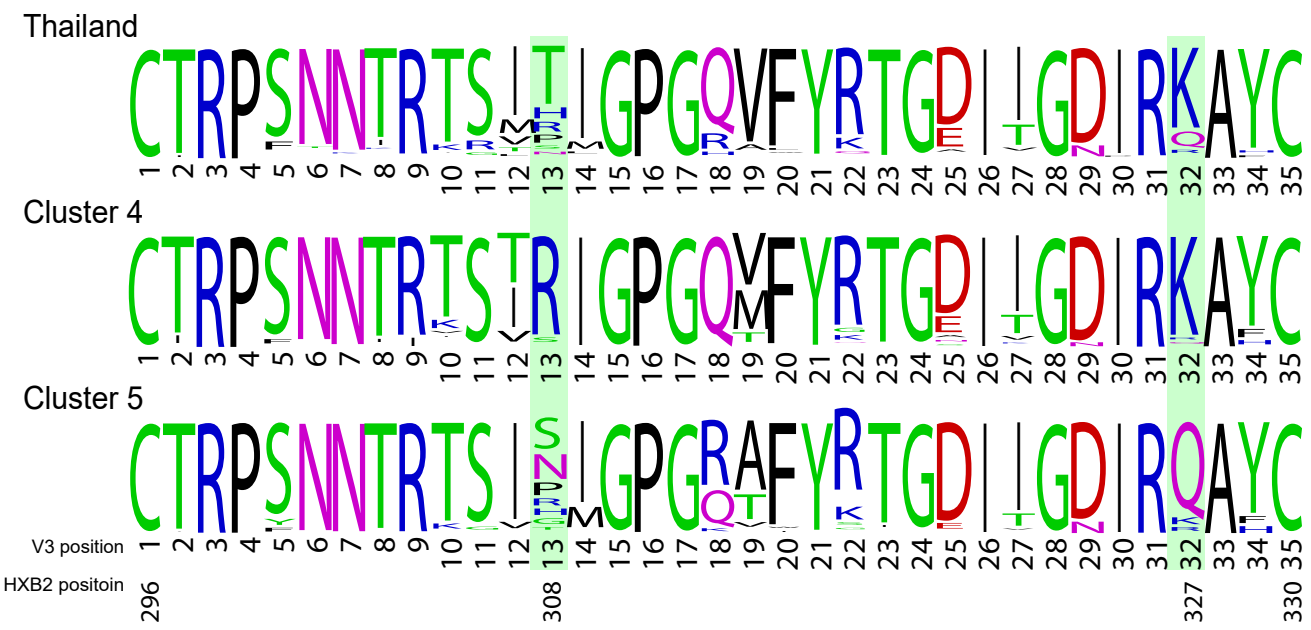


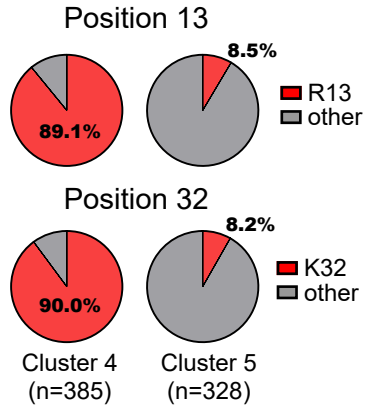
# Figure 4

bioRxiv preprint doi: <https://doi.org/10.1101/427625>; this version posted September 26, 2018. The copyright holder for this preprint (which was not certified by peer review) is the author/funder. All rights reserved. No reuse allowed without permission.

**A**



**B**



**C**

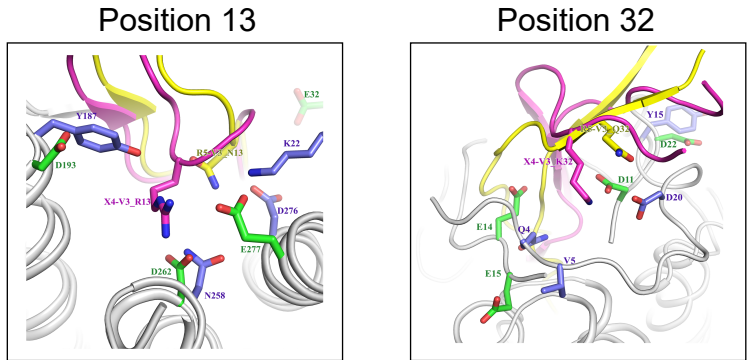


# Figure 5

bioRxiv preprint doi: <https://doi.org/10.1101/427625>; this version posted September 26, 2018. The copyright holder for this preprint (which was not certified by peer review) is the author/funder. All rights reserved. No reuse allowed without permission.

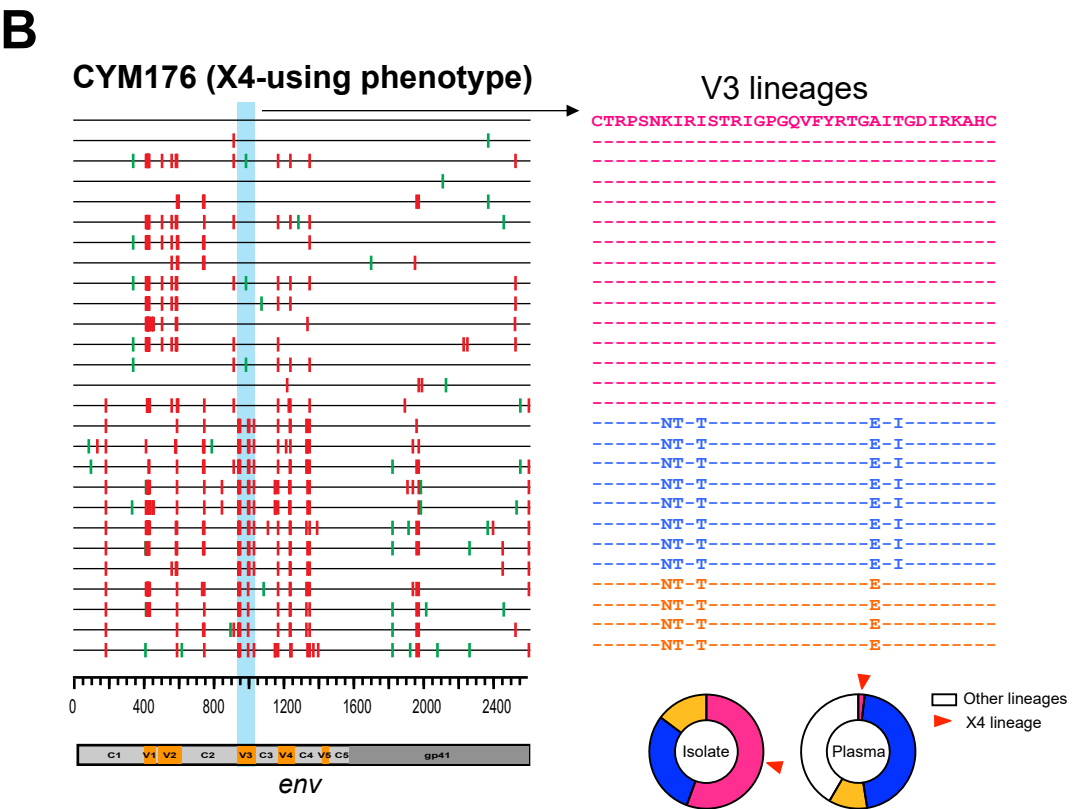
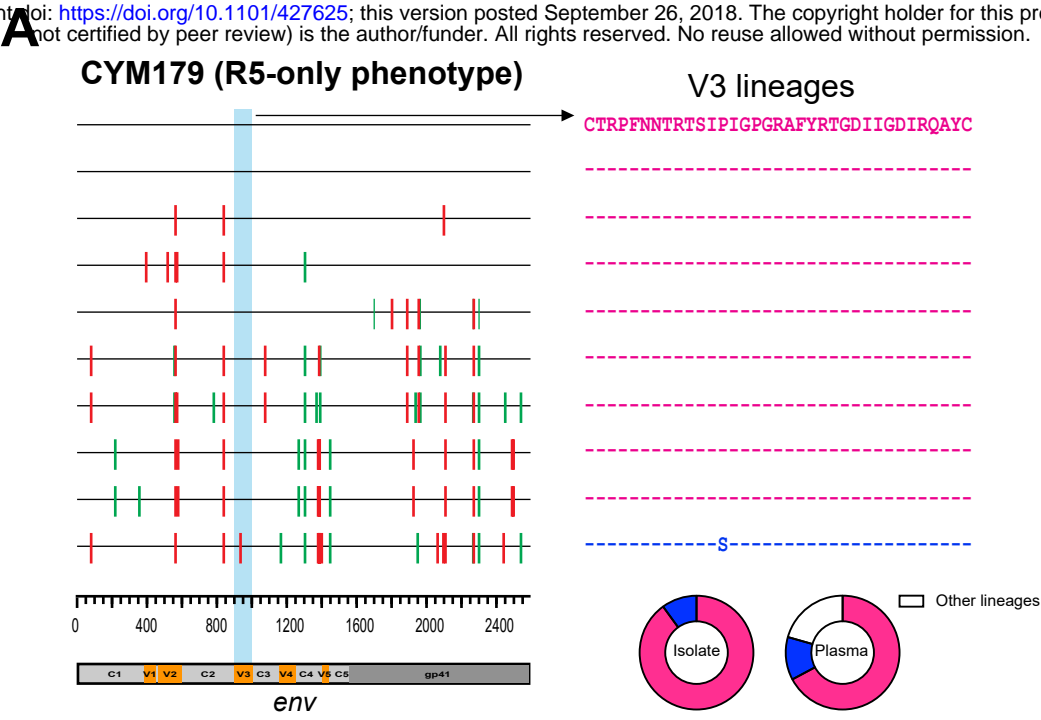


# Figure 6

bioRxiv preprint doi: <https://doi.org/10.1101/427625>; this version posted September 26, 2018. The copyright holder for this preprint (which was not certified by peer review) is the author/funder. All rights reserved. No reuse allowed without permission.

## A

V3 alignment position

← N-glycan →

Subjects	1	2	3	4	5	6	7	8	9	10	11	12	13	14	15	16	17	18	19	20	21	22	23	24	25	26	27	28	29	30	31	32	33	34	35	FPR	Net charge		
<b>Cluster 4</b>	CYM245	C	T	R	P	S	N	K	I	R	I	S	T	R	I	G	P	G	Q	V	F	Y	R	T	G	S	I	L	G	D	I	R	K	A	Y	C	0.2%	6	X4-using
CYM176	C	T	R	P	S	N	K	I	R	I	S	T	R	I	G	P	G	Q	V	F	Y	R	T	G	A	I	T	G	D	I	R	K	A	H	C	0.2%	7		
CYM270	C	T	R	P	S	T	K	I	R	A	S	M	R	I	G	P	G	R	V	F	H	S	T	E	G	I	N	G	D	I	R	K	A	Y	C	0.2%	6		
CYM194.1	C	T	R	P	S	N	K	I	R	T	S	L	R	I	G	P	S	A	V	F	Y	R	T	G	D	I	I	G	D	I	R	K	A	Y	C	0.5%	5		
CYM194.2	C	T	R	P	S	N	K	I	R	T	S	L	R	I	G	P	S	A	V	F	Y	R	T	G	D	I	T	G	D	I	R	K	A	Y	C	0.5%	5		
CYM248	C	T	R	P	S	N	I	M	R	T	P	T	R	I	G	P	G	Q	V	F	Y	R	T	G	A	I	T	G	D	I	R	K	A	H	C	1.3%	6		
CYM279	C	T	R	P	S	N	N	T	R	T	S	T	R	I	G	P	G	Q	V	F	Y	R	T	G	E	I	I	G	D	I	R	K	A	H	C	2.6%	5		
CYM240	C	T	R	P	S	N	N	T	R	T	S	T	R	I	G	P	G	Q	V	F	Y	R	T	G	E	I	I	G	D	I	R	K	A	H	C	2.6%	5		
CYM182	C	T	R	P	S	N	N	T	R	T	S	T	R	I	G	P	G	Q	V	F	Y	R	T	G	E	I	T	G	D	I	R	K	A	H	C	2.8%	5		
CYM286	C	T	R	P	S	N	N	T	R	T	S	T	R	I	G	P	G	Q	V	F	Y	R	T	G	D	I	I	G	D	I	R	K	A	H	C	2.9%	5		
CYM252	C	T	R	P	S	N	N	T	R	K	S	T	R	I	G	P	G	Q	M	F	Y	R	T	G	D	I	I	G	D	I	R	K	A	Y	C	4.8%	5		
CYM280	C	T	R	P	S	N	N	T	R	T	S	T	R	I	G	P	G	Q	M	F	Y	R	T	G	D	I	I	G	D	I	R	K	A	Y	C	5.4%	4		
CYM223	C	T	R	P	S	N	N	T	R	M	S	T	R	I	G	P	G	Q	M	F	Y	R	T	G	D	I	I	G	D	I	R	K	A	Y	C	6.6%	4		
CYM243	C	I	R	P	F	N	N	T	R	T	S	I	R	I	G	P	G	Q	M	F	Y	R	T	G	D	I	I	G	D	I	R	K	A	H	C	9.0%	5		
CYM178	C	T	R	P	S	N	N	T	R	T	S	I	R	I	G	P	G	Q	L	F	Y	R	T	G	D	I	I	G	N	P	R	K	A	Y	C	10.5%	5		
CYM171	C	T	R	P	S	N	N	T	R	T	S	I	R	I	G	P	G	Q	M	F	Y	R	T	G	D	I	I	G	D	I	R	K	A	Y	C	24.7%	4		
CYM249	C	T	R	P	S	N	N	T	R	T	S	I	R	I	G	P	G	Q	M	F	Y	R	T	G	D	I	I	G	D	I	R	K	A	H	C	30.1%	5	R5-only	
<b>Cluster 5</b>	CYM250	C	T	R	P	S	N	N	T	R	T	S	V	R	I	G	P	G	S	T	F	Y	R	T	G	D	I	I	G	D	I	R	K	A	Y	C	11.5%		4
CYM179	C	T	R	P	F	N	N	T	R	T	S	I	P	I	G	P	G	R	A	F	Y	R	T	G	D	I	I	G	D	I	R	Q	A	Y	C	26.3%	3		
CYM186	C	T	R	P	S	N	N	T	R	T	S	I	R	I	G	P	G	Q	T	F	Y	R	T	G	D	I	I	G	D	I	R	Q	A	Y	C	58.3%	3		
CYM293	C	T	R	P	S	N	N	T	R	T	S	I	P	M	G	P	G	R	A	F	Y	R	T	G	D	I	I	G	D	I	R	Q	A	Y	C	60.1%	3		
CYM215	C	T	R	P	S	N	N	T	R	T	S	I	P	I	G	P	G	R	A	F	Y	R	T	G	D	I	I	G	D	I	R	Q	A	Y	C	65.4%	3		
CYM167	C	T	R	P	S	N	N	T	R	E	S	I	N	I	G	P	G	R	A	F	Y	R	I	G	D	I	I	G	D	I	R	Q	A	F	C	71.8%	2		
CYM255	C	T	R	P	S	N	N	T	R	T	S	I	S	I	G	P	G	Q	K	F	Y	R	T	G	D	I	I	G	D	I	R	Q	A	Y	C	73.1%	3		
CYM192	C	T	R	P	S	N	N	T	R	K	S	I	N	I	G	P	G	Q	A	F	Y	Q	T	G	D	I	I	G	D	I	R	Q	A	Y	C	91.3%	2		

## B

